ANNUAL REPORT

1987

CORROSION RESEARCH

Materials Science and Engineering

published
by
THE CORROSION RESEARCH GROUP

FACULTY OF ENGINEERING
HOKKAIDO UNIVERSITY

NO. 16 DECEMBER 1987

For additional copies and more information, please write to the editors ;

Professor T. Ishikawa, Electrometallurgy Laboratory,
Professor N. Sato, Electrochemistry Laboratory,
Professor T. Morozumi, Nuclear Reactor Materials Laboratory

Faculty of Engineering, Hokkaido University, Kita 13, Nishi 8,
Kita-ku, Sapporo 060, Japan

CONTENTS

Passive Film and Anodized Oxide Film

Surface Analysis

Electrometallurgy

Oxidation and Sulfidation

Miscellaneous

ELECTROCHEMISTRY LABORATORY

Prof. Dr. N. Sato, Assoc. Prof. Dr. M. Seo,
Assoc. Prof. Dr. T. Ohtsuka,
Mr. K. Azumi and Miss. J. Fujiwara

Visiting Professor

Prof. Dr. B. Lopez de Mishima

Students

X. C. Jiang, K. Takemasa, H. Bogaki, K. Aotsuka, I. Takeda,
T. Sakamoto, F. Itaya and Y. Haga

The research activity of the laboratory continues to be directed towards a better understanding of the properties of interfacial phase on the surface of metals in relation to the corrosion and passivation of metals and to the interfacial electrochemistry.

Piezo-electric Response to Metal Electrodes

The piezo-electric signals of gold electrode in sulfuric and perchloric acid solutions containing different amount of Cu^{2+} ions were detected to investigate an underpotential deposition of Cu^{2+} ions. The potential of zero charge (PZC) of gold electrode was measured as a function of surface coverage of copper atoms, θ_{Cu} from the piezo-electric signal curves. The drastic change of PZC was observed at $\theta_{Cu}=0.42$, suggesting the surface phase change due to surface reconstruction. Further experiments are continued for the deep insight into the underpotential deposition.

Moreover, the photoacoustic signals of gold, copper and iron electrodes were also measured by piezo-electric response. It is found that the photoacoustic signals depend on the thickness, composition and structure of the surface oxide films. Particularly, the layer structures of passive films on iron and copper electrodes were evaluated from the changes in photoacoustic signals during cathodic reduction of the passive films.

Metal Oxide Films Prepared with MOCVD

Metal oxide films (Cr_2O_3 and Fe_2O_3) and their multilayer films were prepared on platinum substrate with a metal organic chemical vapor deposition (MOCVD). The structural and compositional changes of these films due to heat-treatment in air were measured by Auger electron spectroscopy combined with argon-ion sputter-etching technique and laser Raman spectroscopy. It is found that the structural and compositional changes due to heat-treatment sensitively reflect on the electrochemical characterisctics of the films. The surface coating of MOCVD films on several metals is being examined for improvement of the corrosion resistivity and surface property.

Application of Quartz Crystal Microbalance to Corrosion

Technique of quartz crystal microbalance (QCM) has been applied to an atmospheric corrosion of electroplated copper film. The corrosion rate of copper film in air containing a small amount of H_2S (20 ppm) was measured as a function of relative humidity from the frequency change of QCM. An in-situ gravimetry of palladium electrode by QCM is also being conducted to understand the hydrogen absorption mechanism.

Electroluminescence from Silicon Electrode

Electroluminescence was detected from n type or p type silicon electrode during anodic oxidation in ethylene glycol solution containing NO_3^- ions. The light intensity of electroluminescence increased with increasing anodic current and anodic potential, depending on the semiconductive properties of silicon. The mechanism of electroluminescence is being investigated in relation to the defective structure of anodic oxide films.

Laser Raman Spectroscopy for the Study on Thin Oxide Films on Metals

Characterization in composition of the thin oxide films on metals was conducted by the laser Raman spectroscopy.

The rust layers formed on the weathering steels at 50–100 °C was investigated as a function of exposure period of time, anion contained by thin layer of aqueous solution on the steels, and temperature. The identification of the rust composition by the laser Raman spectroscopy at 50°C showed that the initial layer of γ-FeOOH changes with the exposure time to α-Fe_2O_3, γ-Fe_2O_3, Fe_3O_4, and β-FeOOH, depending on the elements contained by steels and on anions contained by the aqueous solution. The rust layer formed on the steels at 80°C was found to be composed of Fe_3O_4.

The manganese dioxide anodically formed on platinum was also investigated during the discharge process in neutral aqueous solution by the in-situ laser Raman spectroscopy. The Raman peaks changes in intensity and in position with the cathodic potential. The transition of Raman peaks was investigated as a function of the cathodic potential and the cathodic charge.

Osmotic Transfer of Ions Through a Poly-Pyrrole Membrane

Ion-gated composite poly-pyrrole membrane was made as a trial. AC conductance change through the poly-pyrrole membrane was detected, responding to the oxidation and reduction of the poly-pyrrole.

Semiconductive Property of the Passive Film Formed on Titanium

Passivated titanium electrodes in neutral borate and phosphate solutions were measured by using an impedance technique. Dielectric constant of the passive film was obtained as a function of the film formation potential. The property of the passive film as an n-type semiconductor was also investigated. The donor density in the film obtained decreases with increasing thickness of the film, probably because crystallization of the film proceeds. When breakdown of the passive film occurs at the higher potential, the donor density increases again. It is considered that intergap states can be formed with aging time under potentiostatic condition, being then followed by the breakdown of the passive film.

Surface Coating Film by Using the Langmuir-Blodgett Technique

Formation of a very thin polymer film on electrode surface has been tried by using a Langmuir-Blodgett film technique. A surface pressure vs. area curve of a mono-molecule layer of olein acid was studied to check the quality of the apparatus. Photo-polymerization of an diacetylene compound monolayer or a layered film transfered on to a platinum electrode are being examined.

Other Activities

In 1987, Dr. M. Seo attended the European Corrosion Meeting held in Karlsruhe, FRG on April 6–10 and afterwards visited Professor H. -H. Strehblow at the Düsseldorf University and Professor K. E. Heusler at the Technical University of Clausthal. Furthermore, Dr. M. Seo visited Dr. G. Hultquist and Professor J. C. Eriksson at the Royal Institute of Technology in Stochholm, Sweden from April 17-May 5 for a Japan-Sweden collaborative research and also visited Professor I. Olefjord at the Chalmers University of Technology, Goteborg, Sweden.

Dr. M. Seo attended the 4th International Conference on Solid Films and Surfaces held in Hamamatsu, Japan on August 23–27 and presented a paper entitled “Depth-profiling of Metal Oxide Films Prepared with MOCVD”.

Prof. N. Sato, Prof. B. A. Lopez de Mishima and Dr. T. Ohtsuka attended the 172nd Meeting of the Electrochem. Soc. held in Hawaii from the 18th to the 23rd, October, 1987 and presented three papers entitled “The Electrochemical Response of Manganese Hydroxide-Oxide Films in Slightly Alkaline Soluton”, “On Two-layer Growth of Anodic Oxide Film on Cobalt”, and “Laser Raman Spectroscopy Applied for Identification of Iron Rust”.

Dr. M. Seo attended the 10th International Congress on Metallic Corrosion held in Madras, India on November 7–11 and presented a paper entitled “The Effect of Copper-addition on Electrochemical Behavior and Surface Composition of Ferritic Stainless Steel in Sulfuric Acid Solution”.

Prof. B. A. Lopez de Mishima left for Argentina at the beginning of December after a collaborative research on electrochemistry of manganese oxide films for one year in this laboratory.

The following scientists from over the sea paid the short visit to this laboratory in this year of 1987 : Professor E. Gileadi from Tel Aviv University, Israel on May 12, Professor B. Holmstrom from Chalmers/University of Goteborg, Sweden on October 9, Professor C. V. D'Alkaine from Universidade Federal de Sao Carlos, Brazil on November 16-18 and Dr. G. Hultquist from the Royal Institute of Technology, Sweden on November 23-25, 1987.

Oral Presentation

Frequency Dependence of Piezo-electric Response on Surface Stress Change in Gold Electrode ; X. C. Jiang, M. Seo and N. Sato : The 14th Hokkaido Section Meeting of Electrochem. Soc. Jpn., Jan., 1987

Impedance of Anodic Oxide Film on Titanium in Neutral Solution ; K. Azumi, T. Ohtsuka and N. Sato : *ibid.*, Jan., 1987

Surface Composition of Fe-26Cr Alloy in High-Temperature-High Pressure Aqueous Solution ; M. Seo, A. Yamakawa and N. Sato : The 22nd Annual Meeting of the Corrosion Research Association in Hokkaido, Jan., 1987

Passivation of Fe, Co, and Ni ; T. Ohtsuka and N. Sato : *ibid.*, Jan., 1987

Laser Raman Spectroscopy as a Characterization Method of Corrosion Products on Metals ; T. Ohtsuka and N. Sato : The 1986 Winter Meeting of the Hokkaido Section of the Jpn. Soc. for Analytical Chem. and Jpn. Chem. Soc., Feb., 1987

Piezo-electric Response to Surface Stress Change in Gold Electrode and its Frequency Dependence ; X. C. Jiang, M. Seo and N. Sato : The 54th Meeting of Electrochem. Soc. Jpn., April, 1987

An Application of Laser Raman Spectroscopy for the Metallic Corrosion ; T. Ohtsuka and N. Sato : *ibid.*, 1987

Interfacial Study of Metal Electrodes by Piezo-electric Response ; M. Seo : Seminar at Inst. Phys. Chem. (II), Univ. of Düsseldorf, Düsseldorf, FRG, April, 1987

Piezo-electric Detection of Surface Stress Change of Metal Electrodes; M. Seo: Seminar at Dept. of Eng. Metals, Chalmers Univ. Tech., Goteborg, Sweden, April, 1987

Analysis of Initial Surface Oxide Films on Fe–26Cr Alloy in High-Temperature-Borate Solution; M. Seo, A. Yamakawa and N. Sato: '87 Spring Meeting of the Jpn. Soc. Corros. Eng., May, 1987

On the Two-Layered Growth of Anodic Oxide Film on Cobalt; T. Ohtsuka and N. Sato: *ibid.*, May, 1987

Study of the Surface States in the Passive Film formed on Iron; K. Azumi, T. Ohtsuka and N. Sato: *ibid.*, May, 1987

Anodic Polarization Behaviors and Surface Enrichment of Alloying Elements of Stainless Steels in Acidic Aqueous Solution; K. Aotsuka, M. Seo and N. Sato: '87 Summer Meeting of the Hokkaido Section of Jpn. Chem. Soc., July, 1987

Depth Composition Profiles of Thin Metal Oxide Films Prepared with MOCVD; K. Takemasa, M. Seo and N. Sato: *ibid.*, July, 1987

In-situ Raman Spectroscopy of the Manganese Dioxide During the Discharge Process; B. A. Lopez de Mishima, T. Ohtsuka and N. Sato: *ibid.*, July, 1987

Depth-profiling of Metal Oxide Films Prepared with MOCVD; M. Seo, K. Takemasa and N. Sato: 4th International Conference on Solid Films and Surfaces, Hamamatsu, Japan, August, 1987

AC Impedance Characterization of Anodic Dissolution and Passivation; T. Ohtsuka, The 71th Corrosion Symposium of the Jpn. Soc. Corros. Eng., Sept., 1987

Anodic Dissolution and Passivation of Nickel by Piezo-electric Response to Surface Stress Change; M. Seo, X. C. Jiang and N. Sato: The 34th Symposium on Corrosion and Protection, October, 1987

The Electrochemical Response of Manganese Hydroxide-Oxide Films in Slightly Alkaline Solution; M. H. Ubeda, H. Mishima and B. A. Lopez de Mishima: The 172nd Meeting of the Electrochem. Soc., Honolulu, Hawaii, October 1987

On Two-Layer Growth of Anodic Oxide Film on Cobalt; T. Ohtsuka: *ibid.*, October, 1987

Laser Raman Spectroscopy Applied for identification of Iron Rusts; T. Ohtsuka and N. Sato: *ibid.*, October, 1987

The Effect of Copper-addition on Electrochemical Behaviour and Surface Composition of Ferritic Stainless Steel in Sulfuric Acid Solution; M. Seo, J. Guo, G. Hultquist, C. Leygraf and N. Sato: 10th International Congress on Metallic Corrosion, Madras, India, November, 1987

Hydrogen Evolution Kinetics in Corrosion of Copper, Iron and Zinc in Water; M. Seo, G. Hultquist, L. Grasjo and N. Sato: 10th International Congress on Metallic Corrosion, Madras, India, November, 1987

NUCLEAR REACTOR MATERIALS LABORATORY

Prof. Dr. T. Morozumi, Assoc. Prof. Dr. H. Ohashi
Dr. T. Mizuno, Dr. M. Moriya, Mr. K. Hirohara
and Mrs. N. Ochiai

Students

J. Kitabuki, T. Kozaki, T. Fujii, Y. Hayashi,
T. Kimura and N. Mura

The laboratory is concerned with investigations on corrosion of metallic materials used in nuclear industry, characterizations of iron rust components, chemistry of uranium compounds, development and improvement of hydrogen reservoir alloys, and development of computer-aided, electrochemical measurement methods.

The following research is complete or in progress:

(1) Corrosion of SUS304 stainless steel was electrochemically investigated in aqueous solutions of organic chelating reagents which are used for decontamination of primary water coolant circuits of nuclear reactors.

(2) Magnetite and nickel ferrite were synthesized under various conditions by several methods, and characterized by XRD, SEM, Mössbauer spectroscopy and surface area measurement. The dissolution rates of these compounds were measured in aqueous solutions of four kinds of decontamination reagents, EDTA, EDTA+N_2H_4, $H_2C_2O_4$, and $H_2C_2O_4+N_2H_4$.

(3) The ionic strength dependency of the stability constants of uranyl chloro-complex was interpreted by the outer-sphere complex model proposed by Fuoss and Eigen.

(4) Equilibrium and kinetic measurements were made for the hydrogen absorption and release in an $FeTi_{1.1}$ hydrogen reservoir alloy, and the behaviors were explained by the special features of the alloy microstructure.

(5) Anti-pulverization of the $FeTi_{1.1}$ hydrogen reservoir alloy by

electroless plating of copper was investigated. The effective thickness of the plating was determined as a function of alloy particle size. The effectiveness of manganese addition was also evaluated.
(6) The investigation was continued on a computer-aided method devised to observe and analyze various types of electrochemical transients. Under the control of a micro-processor, a cyclic potentiostatic polarization was given to an electrode, and transient response data were obtained for $10^{-5} \sim 10^{2}$ sec time range. A unique analysis method was proposed to obtain the kinetic parameters from these data.

Professor Donald R. Olander from the University of California, Berkeley, visited to our laboratory on June 4, 1987, and gave a lecture on "High-Temperature Behavior of Nuclear Reactor Fuel Elements under Severe Fuel Damage Conditions", to the joint meeting of the Hokkaido Section of the Atomic Energy Society of Japan, the Hokkaido Section of the Japan Institute of Metalls, and the Hokkaido Corrosion Research Association.

Oral Presentations

Changes in Morphology and Dissolution Behavior of Magnetite Under Various Formation Conditions; H. Ohashi, N. Kozai, T. Kozaki, N. Miyazawa and T. Morozumi: The 22nd Annual Meeting of the Hokkaido Corrosion Research Association, Jan., 1987.

Collimator Efficiency in Laser Vaporizing Systems; H. Ohashi, S. K. Yagnik and D. R. Olander: The 1987 Winter Meeting of the Hokkaido Sections of the Chemical Society of Japan and the Japan Society for Analytical Chemistry, Feb., 1987.

Equilibrium Characteristics of Hydrogen Absorption and Release in $FeTi_{1.1}$ Reservoir Alloy; T. Morozumi, K. Ito and T. Mizuno: *ibid.*, Feb., 1987.

Kinetics of Hydrogen Absorption in $FeTi_{1.1}$ Reservoir Alloy; T. Morozumi and K. Ito: *ibid.*, Feb., 1987.

Collimator Efficiency in Laser Vaporizing Systems; H. Ohashi, S. K. Yagnik and D. R. Olander: The 1987 Annual Meeting of the Atomic Energy Society of Japan, Apr., 1987.

Energy and Electrochemistry ; T. Mizuno : The Spring Lecture Meeting of the Hokkaido Institute of Technology, May, 1987.

Behavior of Metallic Materials in vivo Environments ; T. Mizuno : The Meeting of Hokkaido Kyohenkai Association, Apr., 1987.

The Fundamental Knowledge of the Environmental Radiation Monitoring— Where do they come from ? Radiation and Radioactivity in the Environment ; T. Morozumi : The Lecture Meeting of the Hokkaido Nuclear Environmental Center, July, 1987.

Catalyst Regeneration ; M. Tamayama, A. Nishijima and T. Morozumi : China-Japan-U.S.A. Catalysis Symposium, Aug., 1987.

New Technologies and Analytical Chemistry for the 21st Century ; T. Morozumi : The Open Seminar of the Hokkaido Section of the Japan Society for Analytical Chemistry, Sept., 1987.

ANALYTICAL CHEMISTRY LABORATORY

Prof. Dr. R. Furuicihi, Assoc. Prof. Dr. H. Tamura,
Dr. H. Takahashi, Dr. H. Konno
and Miss A. Akazawa

Students

T. Oda, S. Kitazaki, T. Tatsumi, S. Hashimoto
and N. Wakabayashi

Our proposal of purchasing a new ESCA apparatus was approved by the Mimistry of Education. The apparatus, designed by Dr. Takahashi and Dr. Konno consists of a SAM and SAX coupling through a preparation chamber, and is fully computerized. The instrument is now under manufacture at VG company in England. It will be set up in our laboratory in 1988.

Prof. Attila Vértes of Eötvös University, Budapest, Hungary, visited our laboratory in April and gave lectures on Mössbauer Spectroscopy.

Dr. Konno attended the 171st ECS Meeting in Philadelphia in May.

Drs. Tamura, Takahashi and Konno attended the 1987 Japan-US ECS Joint Meeting in Honolulu in October as members of the Hokkaido section of ECS Japan. Dr. Tamura also attended the 3rd Battery Material Symp. in Honolulu.

The following research programs are complete or in progress.

(1) Reaction between metal oxide powders.

The effect of the mixing ratio of oxides on the powder reaction rates was examined for Fe_2O_3-MgO and Fe_2O_3-ZnO systems. The rate of reaction for the V_2O_5-Fe_2O_3 system was measured to check the effect of mixing method on the oxides.

(2) Characterization of acid-base and ion-adsorption behavior of metal oxides in aqueous media.

Acid-base and ion-adsorption phenomena were studied to characterize MnO_2 as dry cell material and Fe_3O_4 as a corrosion product of iron and steel. The phenomena were modeled by considering the stochiometry and equilibrium conditions of reactions. The derived mathematical equations were fitted to experimental data and the equilibrium constants were determined by non-linear regression analysis. The equilibrium constants obtained can be used for predicting the phenomena and for characterizing the oxide samples.

(3) Electrochemical formation of reactive element-Cr composite oxide film on metals.

A method for producing thin composite oxide films of Zr-Cr, Ti-Cr, Ce-Cr and so on was developed. The treated stainless steels showed good oxidation resistance in air containing 20% water vapor at 1273 K, and in air after thermal cycles, 20 h at 1173 K and 4 h at room temperature. The project continues under a grant in aid for scientific research from the Ministry of Education.

(4) High temperature oxidation of stainless steels in H_2O/O_2 atmospheres.

A large amount of data was accumulated for oxidation of Type 430 and 304 stainless steels at 1173-1373 K in 0.03-0.20 atm H_2O-0.165 atm O_2-N_2 atmospheres. The project attempts to understand the mechanism of accelerated oxidation by water vapor.

(5) Formation and deterioration of composite oxide films on aluminum.

Composite oxide films were formed by anodizing aluminum covered with a hydrous oxide, and were examined by electrochemical measurements and electron microscopy. The composite oxide was found to consist of two layers. The crystalline oxide layer contained 'voids' which causes a deterioration of oxide on open circuit in water. The deterioration was correlated with the distribution of voids in the oxide.

(6) Anodizing of Cu-Al and Si-Al alloys.

Cu-Al and Si-Al alloys were anodized in a sulfuric acid solution to form porous oxide films. The structure and formation behavior of the oxide film were examined as functions of the content of alloy element (Cu or Al) and anodizing condition.

Oral Presentations

Characterization of MnO_2; H. Tamura, N. Katayama and M. Nagayama: The 13th Meeting of Hokkaido Section of the Electrochemical Society of Japan, Jan., 1987

Formation of Zn-Cr Composite Oxide Films on Stainless Steels by an Electrochemical Method; H. Konno: *ibid.*

Statistical Evaluation of Oxidation Resistance of SUS 430 Stainless Steel at High Temperatures in Water Vapor Atmospheres; I. Saeki, H. Konno and M. Nagayama: The 22nd Anual Meeting of the Hokkaido Corrosion Research Association, Jan., 1987

Structure of the Composite Oxide Films Formed by Anodizing of Heat-treated Aluminum Covered with Hydroxide Films; H. Takahashi and M. Yamagami: *ibid.*

Effect of Preparation Condition of V_2O_5 on the Reduction Rate in V_2O_5-SO_2 System; A. Simizu, S. Kawarai, M. Ono, R. Furuichi and T. Ishii: The 1987 Winter Meeting of Hokkaido Sections of the Japan Society for Analytical Chemistry and the Chemical Society of Japan, Feb., 1987

Effect of Grinding on the Change in Reactivity and Properties of α-Fe_2O_3; S. Nakano, R. Furuichi and T. Ishii, *ibid.*,

Adsorption of Ni^{2+} Ions on MnO_2; N. Katayama, H. Tamura and M. Nagayama: *ibid.*

Structural Change in the Hydroxide Films on Aluminum with Heat Treatment; H. Takahashi and M. Yamagami: *ibid.*

Formation of Zr-Cr or Ti-Cr Composite Oxide Films on Alloys by an Electrochemical Reduction Technique; H. Konno and R. Furuichi: The 75th Meeting of the Metal Finishing Society of Japan, Mar., 1987

Structure of Hydroxide Films Formed on Aluminum by Hot Water Immersion and Its Change with Heat Treatment; H. Takahashi, M. Yamagami and R. Furuichi: *ibid.*

Effect of SiO_2 Addition on the Development of Duplex Structure of Sintered Fe_3O_4; R. Furuichi, K. Niwa and T. Ishii: The 54th Spring Annual Meeting of Japan Chemical Society, Apr., 1987

Effect of the Method of Mixture Preparation on the Rate in CuO-Al_2O_3 and ZnO-Al_2O_3 System; T. Tsuchida, K. Matsui, R. Furuichi and T. Ishii: *ibid.*

Characterization of MnO_2 by Analysing the Behavior of Zn^{2+} Ion Adsorption; H. Tamura, N. Katayama and M. Nagayama: *ibid.*

Electrochemical Formation of Composite Oxide Film on Steels to Improve Oxidation Resistance at Elevated Temperatures; H. Konno: Corrosion Seminar at the Lehigh University, May, 1987

Electrochemical Formation of Zr-Cr and Ti-Cr Composite Oxide Film on Stainless Steels to Improve Oxidation Resistance at Elevated Temperatures; H. Konno: The 171st Meeting of the Electrochemical Society, May, 1987

Improving Oxidation Resistance of Stainless Steels with Composite Oxide Film Coating; H. Konno, I. Saeki and R. Furuichi: FUSHOKU-BOUSHOKU '87, May, 1987

$ZnFe_2O_4$ Formation from α-Fe_2O_3 Prepared from α-FeOOH; H. Endo, R. Furuichi and T. Ishii: The 1987 Summer Meeting of the Hokkaido Sections of Japan Society for Analytical Chemistry and the Chemical Society of Japan, July, 1987

Emanation Themal Analysis of $CaSO_4$ and $BaSO_4$ in Heating Process; T. Takemura, R. Furuichi and T. Ishii: *ibid.*

Formation of Solid Solution in V_2O_5 and MoO_3; K. Sasaki, A. Shimizu, R. Furuichi and T. Ishii: *ibid.*

Problems in Applying the Law of Mass Action to the Ion-Exchange Equilibria; H. Tamura and R. Furuichi: *ibid.*

Adsorption of Zn(II) Ions on MnO_2 from NH_4Cl Solutions; N. Katayama, H. Tamura and R. Furuichi: *ibid.*

Anodic Oxidation Behavior of Al-Si Alloy in a Sulphuric Acid Solution; H. Takahashi, M. Ito, S. Hashimoto and R. Furuichi: *ibid.*

Breakaway during the High Temperature Oxidation of Stainless Steels; H. Konno: The 1987 Summer Seminar of Hokkaido Corrosion Research Association, Aug., 1987

Structure and Property of Oxide Films Formed on Aluminum;

H. Takahashi: Special Seminar at Hitachi Research Institute, Sep., 1987

Formation Mechanism of Composite Oxide Films on Aluminum; Special Seminar at KDK, Sep., 1987

Structural Change in the Composite Oxide Film on Aluminum with Heat Treatment of Pre-formed Hydroxide Films; The 76th Annual Meeting of the Metal Finishing Society of Japan, Sep., 1987

Adsorption of Zn(II) Ions on MnO_2 in NH_4Cl Solitions; N. Katayama, H. Tamura, M. Nagayama and R. Furuichi: The 3rd Battery Material Symposium (Honolulu), Oct., 1987

Characterization of MnO_2 by Determining the Acid-Base Dissociation Constants of Surface Hydroxyl Groups; H. Tamura, N. Katayama, M. Nagayama and R. Furuichi: The 1987 Japan-US ECS Joint Meeting (Honolulu), Oct., 1987

Statistical Evaluation of Breakaway during the Oxidation of Type 430 Stainless Steel in H_2O/O_2 Atmospheres; H. Konno, I. Saeki and R. Furuichi: *ibid.*

Effect of Heat Treatment of Hydroxides on the Formation of Composite Oxide Films on Aluminum; H. Takahashi, M. Yamagami, R. Furuichi and M. Nagayama: *ibid.*

ELECTROMETALLURGY LABORATORY

Prof. Dr. T. Ishikawa, Assoc. Prof. Dr. T. Narita
Dr. T. Notoya, Dr. T. Sasaki
and Mr. S. Konda

Visiting researcher

Mr. Masami Taguchi

Students

K. Miura, S. Kawaziri, H. Takahashi, R. Konno,
M. Shiobara, A. Hori, T. Mitsueda
and N. Yokoyama

All of staff in this laboratory attended the 172nd Meeting of The Electrochemical Society of U. S. A. co-sponsored by The Japan Electrochemical Society and Japan Society of Applied Physics, which was held in Honolulu, Hawaii, October 18–23, 1987. Mr. Taguchi returned to Akita University in February after completing his sabbatical period of 10 months.

Research in progress are as follows.

(1) Laboratory scale tests in bipolar electrode cells for electrowinning of liquid aluminum and its alloys containing titanium are being carried out by using alkali and alkali earth chlorides molten salts containing $AlCl_3$ and/or $TiCl_4$ in the temperature ranges from 700 to 800°C.

(2) Bipolar electrode cell developed for the aluminum electrowinning has been applied to obtain liquid magnesium from the chloride melt at 750°C.

(3) Sulfidation-oxidation behaviors of boiler tubes in atmospheres encountered in oil fired boiler. Sulfidation and reduction behavior of the preformed oxide scales on an Fe–25Cr alloy was investigated at 973 K in the H_2S–H_2 atmospheres.

(3) Ceramics-metal joinings: bonding systems investigated are as follows. Si_3N_4 and Fe-25Cr alloy with Ni-Cu-Ti filler, Al_2O_3 and Ni with Ag-Cu-Ti filler, and ZrO_2 and Cr with Ag-Cu-Ti filler.

(4) Corrosion and inhibition mechanism of copper and its alloys with nitrogen containing organic inhibitors have been investigated by electrochemical techniques, a conventional optical microscope, SEM and EPMA. The accelerated pitting corrosion test cell, developed by BNF Metals Technology Centre, are being applied for determination of the pitting modes.

(5) A stacked rotating bipolar electrode cell is being tested for the electrochemical treatment of dilute cyanide solution containing heavy metals. The fundamental studies on recovery of gallium from Bayer solution are in progress.

(6) In order to elucidate the effect of small gas bubbles in tap water on the corrosion of pipe-line materials, loop-tests of corrosion are carried out under controlled conditions.

Oral Presentation

Electrowinning of Titanium Alloys from Chloride Melts Containing $TiCl_4$; T. Horie, S. Konda, T. Narita and T. Ishikawa: The 13th Hokkaido Section Meeting of Electrochem. Soc. of Japan, Jan., 1987

The Behavior of a Graphite Electrode in Dilute Cyanide Solutions Containing Copper Ion; T. Sasaki and T. Ishikawa: *ibid.*, Jan., 1987

Reduction Behavior of Various Oxidants on the Titanium Surface: M. Taguchi and T. Ishikawa: The 22nd Annual Meeting of the Corrosion Research Association in Hokkaido, Jan., 1987

Development of Liquid Metal Electrowinning Process with Chloride Melt and Bipolar Electrode Cell; S. Konda, T. Narita and T. Ishikawa: The Meeting of Research Projects, Grant-in Aid for Scientific Research (Energy), Feb., 1987

Corrosion Prevention of Brasses in a Solvent Mixture of Benzyl Alcohol and Oleic Acid; T. Notoya and T. Ishikawa: The 1987 Winter Meeting of the Hokkaido Section of Japan Chemical Society, Feb., 1987

Determination of Type II Pitting Corrosion Propensity in Copper Tubes by Using the BNF Electrochemical Cell; T. Notoya and T. Ishikawa: The 54th Spring Meeting of Japan Chemical Society, Apr., 1987

Corrosion Inhibition Mechanisms of Benzotriazole Related Inhibitors and Their Application; T. Notoya: Rust Prevention Seminar of Japan Association of Corrosion Control, Apr., 1987

Thermal Stability of the Bonding Layer Between Si_3N_4 and Fe-25Cr Alloy (Part 2); K. Miura, T. Narita and T. Ishikawa: The 100th Spring Meeting of JIM, Apr., 1987

Electrowinning of Titanium from Chloride Melts; T. Horie, S. Konda, T. Narita and T. Ishikawa: The 54th Annual Meeting of Electrochemical Soc. of Japan, April 1987.

Protection of Brasses and Bronzes in Organic Solvents Containing Unsaturated Organic Compound; T. Notoya and T. Ishikawa: The '87 Spring Meeting of the Japan Society of Corrosion Engineering, May, 1987

Pitting Tendency Tests for Fresh Water with the BNF Electrochemical Cell; T. Notoya: The Corrosion Committee Meeting of JCDA, March, 1987

Case Studies of Type I Pitting Corrosion in Copper Tubes and Pitting Corrosion Prediction by Using BNF Electrochemical cell; T. Notoya: The Hokkaido Section Spring Meeting of JIM, June, 1987

Oxidation-Sulfidation Behavior of Boiler Tubes; H. Takahashi, T. Narita and T. Ishikawa: The Hokkaido Section Spring Meeting of JIM, June, 1987

Development of Electrometallurgical Processes — Invited Paper—; T. Ishikawa: The 19th Annual Meeting of Fused Salt Chemistry: June, 1987

Bondings of Alumina Ceramics and Metals (Part 1); T. Narita and T. Ishikawa: Spring Meetings on The High-Temperature Materials of JSPS, July, 1987.

Sulfidation behaviors of the Boiler Tubes in the Atmospheres Containing Hydrogen Sulfide Gas; T. Narita and T. Ishikawa:

ibid., July, 1987

Effect of Heat Treatment on the Bonding Structures Between the Ceramics and Metals; T. Narita and T. Ishikawa: Joining Section Meeting of JIM, July, 1987

The Effect of Coexisting Substances on Gallium Deposition in Bipolar Solution; T. Sasaki and T. Ishikawa: The 87th Hokkaido Section Summer Meeting of Japan Chem. Soc., July, 1987

Effect of Phytic Acid and Calcium Phytate on Dissolution of Zinc in Neutral Solutions; T. Notoya: The 1987 Summer Meeting of the Hokkaido Section of Japan Chemical Society, July, 1987

Corrosion of Aluminum Brass in Sea Water; T. Notoya: The Corrosion Committee Meeting of JCDA, Sept, 1987

Pitting Corrosion Propensity Tests for Fresh Waters and Their Application; T. Notoya: The 34th Fall Meeting of Japan Society of Corrosion Engineering, Oct., 1987

Potentiostatic Dezincification of Commercial Brasses and its Inhibition by Organic Inhibitors; T. Notoya and T. Ishikawa: 1987 Joint Meeting of Japan Society of Electrochemistry and American Electrochemical Society, Oct., 1987

Under Scale Corrosion at the Surface of Heat Transfer of a Simulated Small Type of Boilers; T. Murogami, Y. Nakatsuka and T. Notoya: The 34th Fall Meeting of Japan Society of Corrosion Engineering, Oct., 1987

Electrolysis of Dilute Cupric Sulfate Solution by a Stacked Rotaing Bipolar Electrode Cell, 120 mm Diameter, 11 Electrode Cell; T. Sasaki and T. Ishikawa: The 172nd Meeting of ECS, Honolulu, Hawaii, Oct., 1987

Some Aspects on the Internal Sulfidation of Fe-Cr Alloys at Low Sulfur Pressures; T. Narita and T. Ishikawa: *ibid.*, Oct., 1987

A Design Principle of Bipolar Electrode Cell for Electrowinning Cell From Chloride Melts; T. Ishikawa, S. Konda and T. Narita: *ibid.*, Oct., 1987

On the Fracture Strength of Joining Si_3N_4 Ceramics and Stainless Steels Using Ti-Cu-Ni Filler; K. Miura, T. Narita, T. Ishikawa: The 101st Fall Meeting of JIM, Oct., 1987

Oxidation-Sulfidation Behavior of Boiler Tubes; H. Takahashi, T. Narita and T. Ishikawa: *ibid.*, Oct., 1987

Rapid Pitting Propensity Tests of Copper Tubes (BNF Electrochemical Cell) and Its Application; T. Notoya: The 27th Meeting of Japan Copper and Brass Research Association, Nov., 1987

Theoretical Approach to Corrosion Resistivity of Alloys

Masahiro Seo and Norio Sato

Langmuir, 3, 917 (1987)

A model is proposed in which the corrosion resistivity of alloys is closely related to the selective dissolution and surface enrichment of alloying elements. The selective dissolution of some alloying elements from a bare alloy surface takes place before the formation of passive film, and the capacity of passivation depends on the surface enrichment of corrosion-resistive alloying elements. It is assumed that passivation commences when the surface concentration of corrosion-resistive alloying elements exceeds a critical level. The kinetics of surface enrichment of alloying elements is derived by taking into account the selective dissolution rate at the alloy surface and the interdiffusion rate in the alloy substrate. Application of the proposed model is made to the understanding of the corrosion resistivity of stainless steels. (English)

The Dissolution Behaviour of Iron, Chromium, Molybdenum and Copper from Pure Metals and from Ferritic Stainless Steels

G. Hultquist, M. Seo, T. Leitner, C. Leygraf
and N. Sato

Corrosion Science, **27**, No. 9, 973 (1987)

Dissolution rates of iron, chromium, molybdenum and copper as pure metals and as components of three ferritic stainless steels in neutral solutions (distilled H_2O and 0.5 M NaCl) and acid solutions (1 M and 9.2 M of HNO_3 and H_2SO_4) are presented. The relative position of dissoliton rates of the elements is in general the same in pure metal and alloy dissolution. Selective dissolution of iron and simultaneous surface enrichment of chromium is observed under all the investigated conditions. A slight surface enrichment of molybdenum is found upon exposure in the neutral and sulfuric acid solutions but not in nitric acid solution. Large amounts of copper are found in the surface of the copper-containing steel exposed to 1 M H_2SO_4. Evidence is presented which shows that an increase in electrolyte volume decreases the thickness and changes the composition of the passive film. It is believed that this hardly ever mentioned effect is due to an increased amount of dissolution of the film components upon increased volume of electrolyte.
(English)

The Effect of Copper-Addition on Electrochemical Behavior and Surface Composition of Ferritic Stainless Steel in Sulfuric Acid Solution

M. Seo, J. Guo, G. Hultquist, C. Leygraf
and N. Sato

Proc. of 10th ICMC, Madras, India, p. 271 (1987)

Electrochemical behaviors and surface composition of ferritic stainless steels containing copper in 1.0 mol dm^{-3} sulfuric acid solution have been investigated to evaluate the effect of copper-addition on the corrosion resistivity of ferritic stainless steel.

The addition of copper suppressed significantly the active dissolution of the steels due to the surface enrichment of metallic copper. It is found that single minor addition of copper has a detrimental effect on the stability of passive film, whereas combined addition of copper and the other alloying elements is capable of avoiding the detrimental effect. (English)

AC Impedance Characterization of Anodic Dissolution and Passivation

Toshiaki Ohtsuka

Report of the 71st Symposium of Corros. Eng.,
Corros. Eng. Jpn., (1987) p. 21

The impedance characterization was reviewed on the anodic dissolution and passivation of pure iron. For the dissolution mechanism of iron electrode, the results obtained by Epelboin et. al and Schweinckert et al was discussed. For the passivation film the relation between the semiconductive property and the electrode impedance was introduced. In conclusion it was stressed that the results obtained by other techniques must be considered in order to discuss well the impedance results. (Japanese)

Cathodic Reduction of Anodic Oxide Films Formed on Titanium

Toshiaki Ohtsuka, Minoru Masuda and Norio Sato

J. Electrochem. Soc., **134**, 2406 (1987)

Cathodic reduction behavior of the anodic oxide film on titanium has been investigated by using ellipsometry combined with electrochemistry. In acidic sulfate solution, the anodic oxide film reductively dissolves into the solution as Ti (III) ion, resulting in the thinning of its thickness without any significant change of the optical property of the remaining film. In neutral phosphate solution, the anodic oxide film absorbs hydrogen in the hydrogen evolution potential region, resulting in a change of the optical property without thinning its thickness. The amount of hydrogen absorbed per unit volume of the film does not depend on the film thickness but on the cathodic potential. The composition change estimated from measurements of anodic charge during the hydrogen release process indicates that the hydrogen absorption begins to occur at about -0.25 V (vs. RHE) and that the anodic film changes in its composition from TiO_2 to TiOOH at -0.9 V. The hydrogen absorption induces a decrease of the refractive index and an increase of the extinction index of the anodic film. (English)

Mott-Schottky Plot of the Passive Film Formed on Iron in Neutral Borate and Phosphate Solutions

Kazuhisa Azumi, Toshiaki Ohtsuka and Norio Sato

J. Electrochem. Soc., **134**, 1352 (1987)

The semiconductive properties of the passive film formed on iron were investigated by measuring the impedance of passivated iron electrodes in neutral borate and phosphate solutions. Mott-Schottky type of plot was applied to the impedance data to obtain the donor density N_D and the flatband potential V_{FB} as a function of film formation potential, oxidation time, and ion species present in the solution. The value of N_D obtained tor the passive film is in the range of $1 \times 10^{26} - 2 \times 10^{27}$ m^{-3} and decreases with increasing formation potential and oxidation time, indicating that the structural and electronic defects in the passive film decrease with increasing film thickness. The value of N_D of the passive film formed in phosphatesolution is greater than that in borate solution. From the fact that when the electrolyte was changed from borate to phosphate solution N_D increased from the value in borate solution to the value in phosphate solution in a time period of about 10^3 s, it is evident that phosphate ions penetrate into the passive film producing a large number of defects. (English)

Dissolution Behavior of Magnetite in Deaerated EDTA Solutions

S. Takasaki, H. Tamura and M. Nagayama

Boshoku Gijutsu, **36**, 91 (1987)

Magnetite particles were dissolved in deaerated EDTA solutions at 80°C for 9 h, and the saturated concentrations of dissolved iron were examined for different pHs (0.6–10) and EDTA concentrations ($0\text{–}3\times10^{-3}\,\mathrm{mol\cdot dm^{-3}}$). In the absence of EDTA the dissolution occurs only below pH 2, but with EDTA the dissolution region widens up to pH 8. From pH 2 to 4, the (total) concentration of dissolved iron reaches 1.5 times that of EDTA added, but from pH 5 to 7, it is equal to the initial EDTA concentration. The dissolution process is found to consist of the following two reactions: (1) the transfer of Fe^{2+} and Fe^{3+} ions from magnetite to the solution, and (2) the chelation of Fe^{2+} and Fe^{3+} ions with EDTA (Y^{4-}) to form $Fe^{II}Y$ and $Fe^{III}Y$. The solubility product of magnetite was estimated as $Ks=[Fe^{2+}]\,[Fe^{3+}]^2/[H^+]^8=10^4\,\mathrm{mol^{-3}\cdot dm^{15}}$, and using this value the (total) concentration of dissolved iron, the sum of the equilibrium concentrations of Fe^{2+}, Fe^{3+}, $Fe^{II}Y$, and $Fe^{III}Y$, was calculated. The results of calculation agree quite well with the experimental findings. (Japanese)

The Effect of Heat Treatment on the Acid-Base Properties of Manganese (IV) Oxide

Hiroki Tamura, Noriaki Katayama, Masaichi Nagayama
and Ryusaburo Furuichi

J. Chem. Soc. Japan., **1987**, 1524 (1987)

Manganese (IV) oxide suspended in aqueous solutions is covered with acid and base surface hydroxyl groups, $\equiv$MnOH(a) and $\equiv$MnOH(b). The hydroxyl groups form negative and positive sites, $\equiv MnO^-$ and $\equiv Mn^+$, on the oxide surface by dissociation.

In this investigation, the difference in the surface concentrations of the charged sites, that is, the surface charge density, σ, was measured by acid-base titration of manganese (IV) oxide samples with and without heat treatment. The pH at which $\sigma=0$ (pzc) was higher for the heat treated sample than for the as received sample. The dissociation constants, K_a of $\equiv$MnOH(a) and K_b of $\equiv$MnOH(b), were derived by considering the electrostatic effect of σ on the dissociation :

$$K_a = \frac{[\equiv MnO^- \cdot Na^+] \cdot a_H}{[\equiv MnOH(a)]\,[Na^+]} \cdot \exp(-A_a \cdot \sigma)$$

$$K_b = \frac{[\equiv Mn^+ \cdot NO_3^-] \cdot a_{OH}}{[\equiv MnOH(b)]\,[NO_3^-]} \cdot \exp(A_b \cdot \sigma)$$

where $\equiv MnO^- \cdot Na^+$ and $\equiv Mn^+ \cdot NO_3^-$ are charged sites to which the cation and anion of supporting electrolyte ($NaNO_3$) are adsorbed, a_H and a_{OH} being activities of H^+ and OH^- ions, and A_a and A_b being constants. The values of K_a, K_b, A_a, and A_b were determined from an analysis of the experimental σ-pH relationships. It is shown that K_a decreases while K_b increases, and A_a and A_b remain unchanged by the heat treatment of the oxide. The pzc is given by $pzc=(pK_a+pK_w-pK_b)/2$, where K_w is the ionic product of water, and p represents $-$log functions. The increase in pzc by the heat treatment is ascribed to both the increase in pK_a and the decrease in pK_b. (Japanese)

Inhibition of the Oxygen Reduction Reaction Using 8-Hydroxyquinoline

H. Leidheiser, Jr., H. Konno and A. Vértes

Corrosion, Vol. **43**, No. 1, pp. 45–50 (1987)

A corrosion-resistant surface is obtained on steel by a two-step anodization process in which 8-hydroxyquinoline (HQ) is added to the borate anodizing bath in the second step. Additional corrosion resistance is obtained in neutral halide media by a chromate post-treatment. It is conjectured that a multilayer structure impedes the flow of electrons necessary for the oxygen reduction reaction, and the surface is inhibited for the cathodic reaction. The high coverage of the iron surface by the organic complex leads to (1) insulation of the iron from the environment and (2) an inhibition of the anodic reaction. (English)

The Effect of Phytic Acid on the Anodic Dissolution of Copper and Copper-Zinc Alloys

Takenori Notoya

Bulletin of the Faculty of Engineering, Hokkaido
University, No. 137, 31 (1987)

The effects of phytic acid ($C_6H_{18}O_{24}P_6$) and calcium phytate ($Ca_6C_6H_6O_{24}P_6$) on anodic dissolution of copper and four different copper-zinc alloys are studied in a sodium borate-boric acid buffer solution at 60°C.

Anodic polarization was made potentiostatically from a corrosion potential up to 0.90 V vs. S. C. E. for copper and 0.50 V for brasses in the unstirred solutions containing phytic acid or calcium phytate. In the presence of phytic acid both inhibition and acceleration of anodic dissolution depending on its concentration and pH of the solution were observed, i. e., copper dissolution was inhibited by phytic acid to an extent less than 10^{-3} M of pH 9.2 solution while it was accelerated in the solutions at lower pHs.

Copper-zinc alloys dissolution was accelerated at more than 10^{-2} M phytic acid for 90/10 brass 10^{-3} M for 80/20 brass, and 10^{-4} M for 70/30 and 60/40 brasses in the pH 9.2 solution. These opposite effects are probably due to the formation of insoluble and soluble chelates of copper-or zinc-phytate on the metal surfaces depending on phytic acid concentration and copper/zinc ratio in the alloys.

The solution saturated with calcium phytate (about 4×10^{-4} M) inhibited the anodic dissolution of both copper and copper-zinc alloys. (Japanese)

Corrosion Inhibition of Brass and Bronze in Organic Solvents with Unsaturated Fatty Acid

T. Notoya

J. Japan Copper and Brass Research Association
Vol. 26 1 (1987)

Some corrosion products prevent contineous flow of ink by clogging within ink-flowing paths in copper alloy ball point pen tips, particularly after a long time of non-use under adverse conditions. Microscopic observation of the ink-path surfaces were roughened by inhomogeneous dissolution, deposition of insoluble corrosion products, and a number of microcracks perpendicular to drilling direction in oxide stripped substrates. In order to improve the performance and extend the service life of ball point pen by preventing the formation of the ink-blocking corrosion products, screening tests of suitable organic inhibitors as ink additives were conducted to reduce corrosion of the tip materials in a simulated solvent in the presence of inhibitors. Effectiveness of the inhibitiors were evaluated by visual observation of immersed brass and bronze surfaces and 30 day weight loss measurements in a mixture of benzyl alcohol (4 parts by volume) and oleic acid (1 part) containing inhibitors under stagnant conditions at 60°C. The inhibitors tested were benzotriazole and three benzotriazole derivatives, two benzimidazoles, mercaptobenzothiazole, phenyl thiourea, dimercaptothiadiazole and dimethyldithiocarbamic acid. It was found that benzotriazole, its methyl- and carboxylic-derivatives, and dimercaptothiadiazole were effective for both brass and bronze in preventing dissolution and formation of clogging masses of the metallic soap in the solvents. (Japanese)

Anodizing of Aluminum Covered with Hydroxide
I. Formation of Hydroxide and Composite Oxide Films

Hideaki Takahashi, Yasutoshi Umehara, Takeshi Miyamoto,
Norifumi Fujimoto and Masaichi Nagayama

J. Metal Finishing Soc. Japan, Vol. 38, No. 2, 67, 1987

Pure aluminum specimens were covered with hydrous oxide films by immersion in boiling distilled water and then anodized galvanostatically in a neutral borate solution at different temperatures to form composite oxide films. The formation behavior of the hydrous oxide and composite oxide films was examined by gravimetry, XPS, chemical analysis and electron microscopy.

It was found that the hydrous oxide films consist of two layers; a fibrous outer layer (thickness $\delta_{h.o}$) and a dense inner layer ($\delta_{h.i}$). The thickness of the outer layer, $\delta_{h.o}$, increased rapidly with time to reach a steady value of ca. 0.3 μm but that of the inner layer, $\delta_{h.i}$, continued to increase gradually after a rapid increase. The hydrous oxide had a chemical composition of $Al_2O_3 \cdot 2.7\,H_2O$ and a density of ca. 2.3 kg/cm^3, both of which did not change with immersion time.

The composite oxide films consisted of two layers; an outer crystalline oxide layer (thickness δ_0) and an inner amorphous oxide layer (δ_i). During anodizing, $\delta_{h.i}$ decreased linearly, and the total thickness, $\delta_0+\delta_i$, increased linearly with t_a. The $\delta_{h.i}$ vs. t_a and $\delta_0+\delta_i$ vs. t_a curves were independent of anodizing temperature, T_a. The outer layer thickness, δ_0, increased with t_a, at a rate increasing with t_a. This behavior was pronounced at higher T_a. The rate of increase in δ_i decreased with t_a, and this also became more pronounced at higher T_a. The electric field supported by $\delta_i+\delta_o$ was found to increase with t_a from 7.7×10^6 to 10.3×10^6 V/cm. This is explained as being due to the formation of the crystalline oxide layer capable of supporting higher electrical field and to the increase in $\delta_o/(\delta_i+\delta_o)$. (Japanese)

Anodizing of Aluminum Covered with Hydroxide
II. Formation Mechanism of Composite Oxide Films

Hideaki Takahashi, Yasutoshi Umehara
and Masaichi Nagayama

J. Metal Finishing Soc. Japan, Vol. 38, No. 4 138, 1987

On the basis of results obtained in a previous investigation, the growth mechanism of composite oxide films formed when anodizing Al covered with hydroxide was discussed by checking the behavior of ion transport, void formation, and current efficiency for oxide formation.

The mechanism that can be supported is as follows : during anodizing hydroxides are dehydrated to form dense crystalline oxides at the hydroxide/oxide interface, and the voids produced at the interface by shrinkage are repaired with new oxide produced by the outward transport of Al^{3+} across the oxide layer. At the same time, an amorphous oxide is formed at the oxide/metal interface, by the inward transport of O^{2-} ions. The amorphous oxide is then transformed to the crystalline oxide with the formation of voids at the amorphous oxide/crystalline oxide interface at a rate increasing with increasing temperature. The voids thus formed are not filled up with Al_2O_3. The transport number of Al^{3+} ions was estimated to be 0.32 and the current efficiency for oxide formation was 1.21. The volume fraction of the voids produced by the transformation of amorphous oxide to crystalline oxide was calculated to be 0.02-0.08, the value of which increases with increasing anodizing temperature.

An alternative mechanism was also considered, in which the transformation of hydroxide to crystalline oxide does not cause any void formation because of rapid rearrangement of atoms, but it seems to be less probable than the first. (Japanese)

Chemical and Electrochemical Modifications of Zinc Using Organic Compounds

H. Konno, Z. Zhu and M. Nagayama

Plating and Surface Finishing, No. **10**, 40 (1987)

Organic compounds, which form insoluble complexes with zinc in aqueous solutions, were used to modify zinc surfaces and improve corrosion resistance. Used with a anodizing process, a film insoluble in organic solvents was produced below a thin alcohol-soluble zinc complex layer. A chemical treatment resulted in a single alcohol-soluble layer suitable for protection during storage or as a primary coating. (English)

Electrochemical Formation of Zr-Cr Composite Oxide Film on Stainless Steels to Improve Oxidation Resistance at Elevated Temperatures

Hidetaka Konno

J. Electrochem. Soc., **134**, 1034 (1987)

An electrochemical method to form Zr-Cr composite oxide film on steels is reported in the present work. The method provides good oxidation resistance to Fe-Cr alloys down to 10% Cr. In principle, it is possible to develop other compositions including, Y (III), Ce (IV), Gd (III), Nb (V), Ti (IV), Al (III), and others. (English)

Porous Anodic Oxide Films on Aluminum —Microstructure, and Formation/Sealing Mechanism—

Masaichi Nagayama and Hideaki Takahashi

J. Metal Finishing Soc. Japan, Vol. 38, 494 (1987)

This paper summarizes our recent results of investigation on porous anodic oxide films on aluminum and complements a previous review paper. Detailed descriptions are provided of (1) the microstructure of the film as a function of anodizing conditions, (2) anodizing current-voltage characteristics, and (3) hot-water hydration (sealing) and acid-dissolution characteristics of the film. The methods of investigation and their significance are explained. (Japanese)

Surface Films on Copper and Copper Base Alloys and Their Protectiveness in Natural Environments

T. Fujii, N. Nishijima, Y. Watanabe T. Tsuji,
T. Notoya and T. Kawashima

Report. Japan Copper Development
Association p. 55 (1987)

Surface layers formed on copper and five copper alloys and their nature have been investigated examining samples exposed to different atmospheres for period of 1-10 years in Sakai city. X-ray diffraction analysis and FT- infrared spectroscopy showed that cuprous oxide Cu_2O and brochantite $Cu_4(SO_4)(OH)_6$ predominate in the patinas in urban area and industrial area, and small amount of anterlite $Cu_3(SO_4)(OH)_4$ was found in the later environment. No malachite $Cu_2(CO_3)(OH)_2$ and atacamite $Cu_2Cl(OH)_3$ were detected. It appears an early corrosion products subsequently converts to patina after about 9 year exposure. (Japanese)

In situ Infrared Spectroscopy of Iridium Oxide

R. O. Lezuna, Keiji Junimatsu, Toshiaki Ohtsuka
and Norio Sato

J. Electrochem. Soc., **134**, 3090 (1987)

The structural change of an electrochemically grown iridium oxide film upon its electrochromic effect has been investigated in 1 N H_2SO_4 and $HClO_4$, using *in situ* electrochemically modulated infrared spectroscopy (EMIRS). Modulation of the main redox couple operating within the film was found to be associated with the appearance of a O–H stretching band at the bleached state, which is similar to that of pseudoböhmite. Likely oxide species at the bleached and the colored states are considered in view of the reported findings. (English)

IR Reflection and Raman Spectroscopies of the Anodic Oxide Films on Tungsten

Toshiaki Ohtsuka, Noboru Goto, Keiji Kunimatsu
and Norio Sato

Ber. Bunsenges. Phys. Chem., **91**, 313 (1987)

In order to understand the mechanism of the electrochromic reactio of hydrated WO_3, the oxide film formed on tungesten in sulphyric and perchloric acid solutions has been studied by in-situ optical techniques. Ellipsometric measurements reveal that the optical property of the film changes from a transparent substance to a coloured substance at a potential of $E=0.50$ V (vs. RHE). The IR reflection absorption spectroscopy (IRRAS) shows that the anodic oxide film is strongly hydrated forming two types of OH bonds, one corresponding to the incorporated H_2O and the other to the OH bonded with tungsten ion. The Raman spectroscopy (RS) shows that the anodic oxide film is an amorphous form of hydrated tungsten oxide including a terminal W(VI)=O bond. The mechanism of electrochromic reaction is discussed on the basis of IR and Raman spectra which change as the potential shifts from the transparent state to the colouring state. The electrochromic process may sart with a reaction between the terminal W=O and the incorporated H_2O : $W(VI)=O+H_2O_{(film)}+e \rightarrow W(V)-OH+OH_{(film)}$. The $OH_{(film)}$ formed reacts in the film with H^+ injected from the acid aqueous solution. (English)

Surface Characterization of Amalgams Using X-ray Photoelectron Spectroscopy

T. Hanawa, H. Takahashi, M. Ota, F. R. Pinizzotto,
J. L. Ferracane and T. Okabe

J. Dental Research, 66 (9) 1470–1478,
September, 1987

This study is the first to report on the use of x-ray photoelectron spectroscopy (XPS or ESCA) for studying the surface films (less than 10 nm thick) of aged amalgams. The concentrations and electron binding energies of the elements on the surfaces of four different amalgams aged for 20 min, one day, seven days, and 30 days were determined quantitatively. For comparison, the bulk compositions of the amalgams aged for seven days were also determined after removal of approximately 5 nm of material from the surface by argon-ion-sputtering.

The XPS data revealed that the surface films of aged zinc-containing amalgams were not a simple oxide but were primarily composed of a (hydrated) tin and zinc oxy-hydroxide, whereas, in the zinc-free amalgams, the surface films were primarily a tin oxide. The concentration of mercury in this thin surface film after aging was depleted. This suggests that tin and/or zinc preferentially diffused to the surface and combined with oxygen, forming a surface film and diluting the mercury concentration in the surface. Another probable explanation for the depleted mercury is that a minimal amount of mercury in the surface film evaporated during the aging.

FTIR Analysis of Hydroxide Films on Aluminum

H. Takahashi, M. Yamagami, R. Furuichi
and M. Nagayama

J. Surf. Sci. Soc. Jpn., 8, 279, (1987)

FTIR spectroscopy was applied to examine the structural changes in hydroxide films on aluminum with heat treatment. The hydroxide films formed by immersing in distilled water at 99.5°C was identified to be pseudoboehmite, showing characteristic absorption peaks at 3300～3100, 1100, and 800～600 cm^{-1}. The absorbance at 3300 cm^{-1} decreased linearly with increasing temperature up to 600°C, and at 1100 cm^{-1} it remained constant until the temperature attained 300°C, and then decreasing steeply to zero at 400°C. These results suggest that pseudoboehmite films change to boehmite by loosing extra water molecules up to 300°C, and that the boehmite transforms into an anhydrous alumina film above 300°C. (Japanese)

Surface Stress Measurement of Solid Electrode

Masahiro Seo

Bulletin of the Japan Institute of Metals,
26, No. 8, 793 (1987)

The article deals with surface stress measurement of solid electrode. The importance of surface stress measurement for interfacial study of solid electrode was emphasized from the viewpoint of surface thermodynamics.

The electrocapillary curves of noble metal electrodes obtained from several methods such as thin film-bending, ribbon extension and piezo-electric response were introduced for deep insight into interfacial phenomena of solid electrodes. Furthermore, the stress components originated from surface oxide films on electrodes were discussed with relation to growth mechanism of oxide films.
(Japanese)

Piezoelectric Response to Surface Stress Change of Gold Eleectrode in Sulfate Aqueous Solutions

Masahiro Seo, Xiang Chun Jiang and Norio Sato

J. Electrochem. Soc., **134**, No. 12, 3094 (1987)

The interfacial properties of gold electrode in sulfate solutions of different pH values have been investigated from the piezoelectric response of surface stress change induced by a potential modulation. The potential of electrocapillary maximum, $E_{\max}$, obtained from the piezoelectric signals is independent of pH in acidic and neutral range but shifts to the less noble direction at pH higher than 8. The piezoelectric signals could sensitively respond to the structual changes of electric double layer which are ascribed to the reorientation of water dipoles in acidic solution and the charge transfer of electrosorbed OH^- ions in alkaline solution. It is expected that the sign of surface charge of gold electrode in alkaline solution changes gradually from plus to minus at the high anodic potential of oxide formation. It seems that the sign reversal of surface charge is associated with the aging process of hydrous oxide, $Au(OH)_3$, initially formed on gold. (English)

Electrolysis of Dilute Cupric Sulfate Solution by a Stacked Rotating Bipolar Electrode Cell, 120 mm Diameter, 11 Electrode Cell

T. Sasaki and T. Ishikawa

Extended Abstracts of the 172nd Fall Meeting
ECS, Vol. 87-2 (1987), 818

The performance of a 120 mm diameter stacked rotating bipolar electrode cell electrolyzing 120 liters of dilute cupric sulfate has been investigated and compared with that from a cell one fourth the size. To attain high current efficiency and low energy consumption without sacrificing too much recovery speed the electrolysis must be carried out with a step-wise decreased current. The electrolysis takes a little longer, but the energy consumption is lower than with the smaller cell. (English)

A Design Principle of Bipolar Electrodes for Electrowinning Cell From Chloride Melts

Tatsuo Ishikawa, Shoichi Konda
and Toshio Narita

Proceedings of the Joint International Symposium
on MOLTEM SALTS, p. 734～743, 1987

A design principle of bipolar electrodes for liquid metal electrowinning cell was discussed theoretically. By taking into consideration of volume balance and homogeneous circulation of the chloride melt, general equations were dedeuced for determination of each sectional area of the bipolar electrodes. The values of design parameters were checked experimentally by operating the laboratory-scale cells constructed with the proposed deisgn principle, in which following variables were supposed to be known ; the number of the inter-spacing reaction zones and a total sectional area of the cell, an average surface are and thickness of the bipolar electrodes, a distance between electrodes, specific conductivity of the chloride melts and decomposition voltage of aluminum chloride in the melt at various concentrations at operational temperatures. (English)

Development of Liquid Metal Electrowinning Process with Chloride Melts and Bipolar Electrode Cell

T. Ishikawa, S. Konda and T. Narita

Reports of Special Project Research on Energy Under
Grant in Aid of Scientific Research of the
Ministry of Education, Science and
Culture, Japan October 1987

From our experimental results on the bipolar electrode cell for electrowinning of liquid aluminum from chloride melts, it had been elucidated to decrease maximum current efficiency attainable with a given bipolar electrode cell and to increase heat loss through cell wall in a large way, owing to the chloride melt permeated into the cell wall. This chloride melt permeation into the cell wall should be reduced as far as possible with the view of industrial application.

Therefore, the wall structures were proposed and their performances were checked with operation of the cell having five units, 550 cm^2 inner area. The cell walls constructed in these laboratory scale tests are an alumina particles-packed type and a quartz tubes-stacked type.

In this report, firstly, it is described the results of thermal conductivity measurement on the above mentioned cell wall without and with the chloride melt permeated in the wall structures. And also is described the electrolytic results obtained with the bipolar electrode cell having quartz tubes-stacked wall. It is concluded that the tubes-stacked wall is a promising wall structure for the industrial application from the view of low electrolytic and thermal conductivity under operating conditions. (English)

Characteristics of a Stacked Rotating Bipolar Electrode Cell for Mass Transfer

Takeshi Sasaki and Tatsuo Ishikawa

Memoirs Fac. Eng. Hokkaido Univ., **17**, 145 (1987)

The characteristics of mass transfer in a stacked rotating bipolar electrode cell was investigated by measuring the diffusion limiting currents at various rotational speeds and flow rates under a variety of heights and numbers of fins with 0.01 M ferri/ferrocyanide in a 1 M NaOH aqueous solution ($M = mol \cdot dm^{-3}$). Three single cells of different sizes were used as model cells of the stacked rotating bipolar electrode cell. The equivalent speed of rotation and the equivalent volumetric flow were determined by matching the diffusion limiting current curves for the three cells.

The mass transfer effect of the agitation by the fins attached to the electrodes is remarkable and the distance of 1 mm from the head of fins to the opposite surface is sufficiently small for the fins to raise the effective agitation. The limiting current is hardly affected by the variation in the fin height and the number of fins. The diffusion limiting current cannot be expressed by a simple function of the rotational speeds and volumetric flow. The reciprocal of the equivalent speed of rotation and the equivalent volumetric flow are linearly related with the rotor radius. (English)

Mass Transfer in a Stacked Rotating Bipolar Electrode Cell

Takeshi Sasaki and Tatsuo Ishikawa

DENKI KAGAKU (J. Electrochem. Soc. Japan),
55, 145 (1987)

The characteristics of mass transfer in a stacked rotating bipolar electrode cell was investigated by measuring diffusion limiting currents under a variety of rotational speeds and flow rates with 0.01 M ferri/ferrocyanide in a 1 M NaOH aqueous solution ($M = mol \cdot dm^{-3}$). Three single cells of different sizes were used as model cells of the stacked rotating bipolar electrode cell. The equivalent speed of rotation and the equivalent volumetric flow, for similar diffusion limiting current densities in the three cells, were determined by matching the diffusion limiting current curves for the three cells. The diffusion limiting current cannot be expressed by a simple function of the rotational speeds and volumetric flow. The mass transfer effect of the agitation by the fins attached to the electrodes is remarkable, especially at the surface of the stator opposite the rotating fins. The reciprocal of the equivalent speed of rotation and the equivalent volumetric flow are linearly related with the rotor radius. (English)

Oxidation Kinetics of Uranium Dioxide

Hiroshi Ohashi, Hideyuki Hayashi, Masahiro Nabeshima
and Takashi Morozumi

Bulletin of the Faculty of Engineering, Hokkaido
University No. 134, 49-57 (1987)

Oxidation rates of three kinds of UO_2 of different particle sizes were thermogravimetrically measured as functions of temperature and oxygen pressure. The weight gain-time curves varied markedly with particle size. The UO_2 microspheres for HTGR oxidized in a single stage from UO_2 to U_3O_8, while the UO_2 powder oxidized in two distinct stages from UO_2 to U_3O_7 and then to U_3O_8. The behavior of the crushed UO_2 microspheres was intermediate to the above two extremes, and the weight gain-time curves had plateaux at compositions below U_3O_7. The phenomena were attributed to the delay of the oxidation from U_3O_7 to U_3O_8. For the powder, the oxidation to U_3O_8 started after UO_2 completely converted to U_3O_7. For the microspheres, the oxidation of UO_2 proceeds inwards from the surface of the spheres with UO_2-U_3O_7 and U_3O_7-U_3O_8 interfaces. Because of the nearly equal linear rates of advancement of these two interfaces, the thermogravimetric oxidation curves show as one stage, as if oxidation directly proceeds from UO_2 to U_3O_8. The steady state thickness of the U_3O_7 layer between UO_2 and U_3O_8 was estimated to be 1-2 μm. Further, α-U_3O_7, β-U_3O_7 and β'-U_3O_7 were identified as intermediate oxidation products and it was concluded that the relative fraction of these products controls the second stage of the oxidation from U_3O_7 to U_3O_8. (Japanese)

Oxidation Properties of Co–Mn Alloys at Temperatures from 1273 to 1473 K

Toshio Narita, Tatsuo Ishikawa, Shun-ichi Karasawa,
and Keizo Nishida

Oxidation of Metals, Vol. 27 (Nos. 5/6),
1987, 267～282

The oxidation behavior of Co alloys containing up to 23.0% Mn was investigated at temperatures of 1273–1473 K in an oxygen pressure range of 10–10^{-5} Pa using thermogravimetry, electron-probe microanalysis, and optical microscopy.

Oxidation followed a parabolic rate law, except in the early reaction stage. For the growth of the (Co, Mn)O scale, parabolic rate constants increased with increasing manganese content, whereas with further additions of manganese the rate constants decreased due to an intermediate layer of $(Co, Mn)_3O_4$. This critical manganese content increased with increasing temperature. The scale structures were classified into three groups: group I, a single-layer scale; group II, an inner-outer double layer; and group III, an inner-intermediate-outer triple layer. The inner layer consisted of (Co, Mn)O; the outer layer was a mixture of (Co, Mn)O and $(Co, Mn)_3O_4$; the intermediate layer was composed of $(Co, Mn)_3O_4$. Cation concentration profiles were measured across the external scales with single- or multilayer structures. Diffusional analysis indicated that manganese moved 1.25 times faster than did cobalt in the (Co, Mn)O scale. Activation energies for oxidation are 118–126 kJ/moles for group I and II, and for the alloys in group III they are 290–367 kJ/moles. Parabolic rate constants and scale structures are discussed on the basic of the Co–Mn–O phase diagram. (English)

Some Aspects on the Internal Sulfidation of Fe-Cr Alloys at Low Sulfur Pressures

Toshio Narita and Tatsuo Ishikawa

Proceedings of the Symposium on High-Temperature
Materials Chemistry-IV, ECS, Vol. 88-5
(1987), 71-79

This is a report of an investigation of diffusional analysis of the kinetics and concentration profiles for sulfidation of Fe-Cr alloys at low sulfur pressures, below the dissociation pressure of ferrous sulfide. The results indicate that the calculated rate constants and concentration profiles were in good agreement with the observed ones, except when internal sulfidation took place. There are two internal sulfidation modes : grain boundary sulfidation is considered an inner scale formation controlled by chromium diffusion from the alloy, and the usual internal sulfidation is explained by assuming an enhanced diffusion flux of sulfur due to sulfur-metal interaction in the alloy phase. This internal sulfidation is typical for medium chromium alloys at 1173 K, and is caused by a change from alpha to gamma phase, which has a very low chemical diffusivity.
(English)

High-Temperature Corrosion of Boiler Tubes in the H_2S-H_2 Gas Mixtures

Toshio Narita, Tatuo Ishikawa, Keizo Nishida
and Shorzi Nakamori

Reports on High Temperature Materials in the
123rd Division of JSPS, Vol. 28
(No. 2), 1987, 239-250

As one of the series of the high temperature corrosion study of boiler tubes, sulfidation behavior of STBA24 and STB42 steels were investigated in H_2S-H_2 gas mixtures at temperatures from 673-973 K.

It was found that both boiler tubes sulfidized relatively rapid, so that sulfidation of these steels in practical problems are expected to be occurred through the oxide and ash deposited scale.

Sulfidation behavior of Fe-2.33Cr, Fe-2.33Cr-1Mo, Fe-1Si and Fe-2Si alloys were investigated for comparison. Addition of chromium and molibdenum do not affect on the sulfidation of pure iron, where silicon caused a remakable decrease in the sulfidation rates. This seems to be due to the formation of the Si-riched surface scale on the alloy surface and inner scale. (Japanese)

Phase Relations in an Fe–Cr–S System at Temperatures of 1073 and 1173 K in the Sulfur Pressure Range from 10^0 to 10^{-5} Pa

Toshio Narita, Tatsuo Ishikawa and Keizo Nishida

Oxidation of Metals Vol. 27 (Nos. 3/4),
1987, 239～252

Phase relations and stability fields in the Fe–Cr–S system were investigated at 1073 and 1173 K in the sulfur pressure range 10^0–10^{-5} Pa. The sulfides, produced by the sulfidation-annealing process of Fe–Cr alloys followed by rapid quenching, were characterized using X-ray diffraction powder analysis at room temperature. The Cr_3S_4 in the Cr–S system extends beyond the $FeCr_2S_4$ stoichiometry in the Fe–Cr–S ternary system at intermediate sulfur pressures. The spinel-monoclinic transition of the $FeCr_2S_4$ was observed at sulfur pressures of 10^{-3}–$10^{-3.5}$ Pa at 1073 K and at 10^0–$10^{-0.5}$ Pa at 1173 K. The free energy change for formation of the spinel, $FeCr_2S_4$, from a monoclinic $(Cr, Fe)_3S_{4-y}$, hexagonal $(Fe, Cr)_{1-x}S$, and sulfur vapor is given by the relation $\Delta G = 1523 + 1.09\,T$ (kJ/mol). The phase-transition mechanism of $FeCr_2S_4$ is discussed on the basis of an enhancement of the cation coordination numbers from 4–6–6 for the spinel to 6–6–6 for the monoclinic, when the sulfur partial pressure decreases. (English)

Sulfidation Kinetics and Scale Structures of Chromium at Temperatures of 973-1173 K and 10^4-10^{-6} Pa Sulfur Pressures

Toshio Narita, Tatsuo Ishikawa and Keizo Nishida

Oxidation of Metals, Vol. 27 (Nos. 3/4),
1987, 221-237

The sulfidation behavior of chromium was investigated over a temperature range of 973-1173 K in H_2S-H_2 gas mixtures of 10^4-10^{-6} Pa sulfur partial pressures using thermogravimetry, X-ray diffractometry, optical and scanning electron microscopy, and electron-probe microanalysis. Sulfidation kinetics are rapid for short periods and obey a linear rate law at low sulfur pressures, whereas at high sulfur pressures sulfidation tends to be parabolic. The surface morphologies can be divided into four types : at high sulfur pressures a petal-like crystal of Cr_2S_3 (rho. and tri.) (type 1), at intermediate sulfur pressures a twinlike structure of Cr_3S_4 (type 2), at low sulfur pressures a flat surface with numerous hexagonal pits of $Cr_{1-x}S$ (type 3), and a fine twinlike structure of ordered $Cr_{1-x}S$ (type 4). At 973 K, the sulfur pressure ranges are type 1 at $p_{S2} > 10^{-4}$ Pa, type 2 at $p_{S2} = 10^{-5}$ Pa, and type 3 at $p_{S2} < 10^{-6}$ Pa. The critical sulfur pressure where type 2 was formed, 10^{-5} Pa at 973 K, shifts toward higher pressures at higher temperatures and becomes 10^{-3} Pa at 1073 K and 10^{-1} Pa at 1173 K. Type 4 is observed at 1173 K and 10^{-6} Pa sulfur pressure. The sulfide scale is composed of two distinct layers : an external layer, which is dense with a fine columnar structure, and an inner layer, which is porous with a layered structure of sulfides and voids. The external scale is composed of four layers at high sulfur pressures : at the scale-gas interface Cr_2S_3(rho.), next Cr_2S_3(tri.), third Cr_3S_4, and innermost $Cr_{1-x}S$. With decreasing sulfur pressures, the number of layers in the external scale was reduced. Pt markers were positioned between the external and inner scales. (English)

Sulfidation Properties of $Cr_{23}C_6$ at 1073 K in H_2S-H_2 Atmospheres of $10^{3.5}$-10^{-6} Pa Sulfur Pressure

Toshio Narita, Tatsuso Ishikawa, Kiyoshi Imai
and Keizo Nishida

Oxidation of Metals, Vol. 28 (Nos. 1/2) 1987, 17~31

The Sulfidation behavior of chromium carbide, $Cr_{23}C_6$, was investigated in H_2S-H_2 gas mixtures over a sulfur partial pressure range of $10^{3.5}$-10^{-6} Pa at 1073 K using thermogravimetry, optical and scanning electron microscopy, X-ray diffraction analysis, and electron-probe microanalysis. The kinetics were rapid for short time periods and followed a linear rate law at low sulfur pressures, whereas sulfidation tends to obey a parabolic rate law at high pressures. Sulfidation rates decreased with increasing carbon content in the carbide. Surface morphologies could be divided into three groups : (I) at high sulfur pressures, petal-like crystals (Cr_2S_3) ; (II) at intermediate pressures, a twinlike structure (Cr_3S_4) ; (III) and at low pressures, a flat surface with numerous hexagonal pits ($Cr_{1-x}S$). The scale consisted of two distinct layers : an external scale with a single or multilayer structure and an inner scale with a mixture of $Cr_{1-x}S$, Cr_3C_2, and Cr_7C_3. These higher carbides, Cr_3C_2 and Cr_7C_3, may be formed by the sulfidation-carburization of $Cr_{23}C_6$. Pt-marker experiments indicated that the external scale grew by chromium diffusion and that sulfur migration played an important role in the growth of the inner scale. (English)

Sulphidation Properties of Chromium and Chromium-containing Alloys at High Temperatures

Toshio Narita and Tatsuo Ishikawa

Materials Science and Engineering,
Vol. 87, 1987, 51～61

The sulphidation behaviour of chromium alloys is reviewed in three different sulphur pressure ranges and the effect of chromium on the sulphidation kinetics and scale structure is discussed. It is generally known that chromium is resistant to sulphidation at high sulphur pressures, while it sulphidizes rapidly at low sulphur pressures. This seems to be due to phase changes from Cr_2S_3 or Cr_3S_4 to CrS_x. At low sulphur pressures, copious internal sulphidation is formed for Ni-Cr alloys whereas, for Fe-Cr alloys, sulphidation is confined to grain boundaries.

The sulphidation properties of chromium and $Cr_{23}C_6$ were investigated at 1073 K in the sulphur pressure range from $10^{3.5}$ to 10^{-6} Pa. Both chromium and $Cr_{23}C_6$ showed similar kinetics and scale structures, except for the formation of Cr_7C_3 in the inner layer of sulphidized $Cr_{23}C_6$. It is concluded that, at the low sulphur pressures which often occur in an internal sulphidation zone, chromium and $Cr_{23}C_6$ sulphidize faster than the alloy substrate and also that the grain boundary sulphidation of Fe-Cr alloys is due to the preferential sulphidation of chromium carbides and not of the chromium-depleted alloy matrix. (English)

Equilibrium Characteristics of Hydrogen Absorption and Release in $FeTi_{1.1}$ Reservoir Alloy

Takashi Morozumi, Kunio Ito and Tadahiko Mizuno

Bulletin of the Faculty of Engineering, Hokkaido
University, No. 134, 59-68 (1987)

Equilibrium isotherms were measured under a variety of experimental conditions during the hydrogen absorption and release processes in a $FeTi_{1.1}$ reservoir alloy, and approximate equations were given for these characteristics. These isotherms exhibited a large hysteresis within a cycle of absorption and release processes, but no perfect horizon was observed in the plateau.

These characteristics were explained by postulating the special nature of the alloy micro-structure, in which storage sites were irregularly distributed with different hydrogen potentials and vacant sites with higher potentials constructed a blockade front line against the penetration of hydrogen atoms into the depth of alloy matrix. From the results of estimation with the above-mentioned equations, it was suggested that a depletion of absorption rate observed at high temperature could be attributed to the decrease of available vacancy. (Japanese)

Kinetics of Hydrogen Absorption in $FeTi_{1.1}$ Reservoir Alloy

Takashi Morozumi and Kunio Ito

Bulletin of the Faculty of Engineering, Hokkaido
University, No. 134, 69-77 (1987)

Kinetic studies were persued on hydriding of non-stoichiometric iron-titanium reservoir alloy, and the effects of temperature and hydrogen gaseous pressure upon the reaction rate were determined. At temperatures above 273 K, the rate changed in a proportional manner to the square root pressure driving force, $P^2-P_e^2$, and the available vacancy density, Δn_{H_2}. As the most plausible mechanism, non-linear diffusion was postulated, in which the diffusion constant varied with Δn_{H_2}. The potential field assisted diffusion with a finite pressure drop was also suggested as another possible mechanism. At $T<263$ K, the rate indicated a dependency of higher order upon both of gaseous pressure and Δn_{H_2}, but the exact explanation was not yet obtained. (Japanese)

The Influence of Preparation Conditions of Powder Mixtures on the Reaction of V_2O_5-Fe_2O_3 System

Akira Shimizu, Ryusaburo Furuichi and Tadao Ishii

Bulletin of the Faculty of Engineering.
Hokkaido University, No. **136**,
99 (1987)

In order to investigate the influence of preparation conditions of powder mixtures on the rate of $FeVO_4$ formation, five mixtures (**M1-M5**) were prepared by using three V_2O_5 **V1**, V2 and **V3**) and two Fe_2O_3 (**F1** and **F2**) powders. **V1** was prepared by thermal decomposition of NH_4VO_3 at 450°C and **V2** and **V3** were prepared from **V1** by manual grinding in a mortar (**V2**) and by jet mull grinding (**V3**), respectively. **F1** and **F2** were prepared from commerical α-Fe_2O_3 by sieving under 325 mesh (**F1**) and by manual grinding in a mortar (**F2**), respectively. Equimolar mictures of these V_2O_5 and Fe_2O_3 were obtained by mixing in an agate mortar for 1 hr with a weak force (**w**) and strong force (**s**) respectively. The preparation conditions of the mixtures are as follows: **M1** (**V1**, **F2**, **w**), **M2** (**V2**, **F2**, **w**), **M3** (**V3**, **F2**, **w**), **M4** (**V2**, **F1**, **w**) and **M5** (**V2**, **F2**, **s**). The rate was evaluated by using Jander's equation ($[1-(1-\alpha)^{1/3}]^2=k_jt$). The order of the rate was $k_{jM5} \simeq k_{jM3} > k_{jM2} > k_{jM4} > k_{jM1}$. Particle sizes ($d$) of V_2O_5 and Fe_2O_3 in the mixtures were $d_{V1} > d_{F1} > d_{V2} = d_{V3} = d_{F2}$. Lattice strain ($\eta_a$) of V_2O_5 was estimated by Hall's plot of (200), (400) and (600) planes. The order of η_a-value of V_2O_5 in the mixtures was found to be $\eta_{aM3} > \eta_{aM5} > \eta_{aM2} = \eta_{aM4} > \eta_{aM1}$. The increase in k_j-value was explained by the increase in η_a of V_2O_5 and in the contact point between reacting particles. (Japanese)

Influence of Preparation Temperatures of V_2O_5 Powder on Reduction Rate in V_2O_5-SO_2 System

Akira Shimizu, Shuji Kawarai, Ryisaburo Furuichi
and Tadao Ishii

Memoirs of the Fuculty of Engineering,
Hokkaido University, Vol. VVII,
No. 2 167 (1987)

Reactivity of three V_2O_5 (**V1**, **V2** and **V3**) obtained at different preparation temperatures (T_p) was compared by their rate of reduction in SO_2 stream of 300 ml/min. The V_2O_5 samples were prepared by thermal decomposition of NH_4VO_3 in air stream of 100 ml/min at 400 (**V1**), 450 (**V2**) and 550°C (**V3**) for 1 hr. The reduction followed Mampel's equation in a temperature range of 350-400°C. The measured rate was decreased with an increase in T_p. SEM observation and measurements of interplanar spacing (d_{hoo}), peak breadth at half maximum intensity (β_{hoo}), BET surface area (S), and stretching vibration frequency of $V=O(\nu)$ of V_2O_5 were carried out. Values of ν and d_{hoo} were independent of T_p. Lattice strain η_a and crystallite size L_a were estimated by Hall's method from β_{hoo}. η_a was decreased with T_p while L_a was increased. L_a agreed with the diameter (D_s) calculated from S. The reduction was presumed to proceed on the surface of V_2O_5 crystallites. The change in the reduction rate with T_p was considered to depend on the strain energy stored in the crystallite. (English)

Effect of the Mixing Ratio of Reactant Oxides on the Rate of Powder Reactions in Fe_2O_3-MeO (Me=Mg and Zn) System

Ryusaburo Furuici, Kazuyoshi Kamada,
Yuji Yoshioka and Tada o Ishii

Bullentin of the Faculty of Engineering,
Hokkaido Univeristy, No. 134,
p. 19 (1987)

Two ferric oxide samples, Fe_2O_3 (I) and Fe_2O_3 (II), prepared from ferric hydroxides were calcined at 500, 700 and 900°C for 3 h and then were sieved between 250 and 325 mesh. These Fe_2O_3 were allowed to react with MgO and ZnO powder (250-325 mesh) at various mixing ratios (r_m) of the reactant oxides.

The value of r_m was represented by the molar fraction of Fe_2O_3 in the mixed sample. A v-shell blender was operated for 2 h to prepare the mixtures of the oxides and a pellet sample was obtained by pressing the mixture (150-300 mg) at 2.7×10^3 kg/cm^2 for 10 min. Isothermal reaction was carried out in air at 800-950°C. The rate of $MgFe_2O_4$ and $ZnFe_2O_4$ formation was found to obey Jander's kinetics, which is based on the diffusion mechanism, but in the case of $ZnFe_2O_4$, an initial rapid surface reaction was suggested to occur before the diffusion process started.

The diffusion rate was observed to change with r_m, that is, the apparent rate constants (k_j or k_{jc}) vs. r_m showed a v-shaped curve with a minimum value near $r_m=0.5$. This fact indicates that the rate depends on the number of contact points between the reactant particles. The rate constants k_A^O and k_B^O were calculated ; the former is the value corresponding to the situation where MgO (or ZnO) particles are surrounded by only Fe_2O_3 particles and the latter corrosponds to that where Fe_2O_3 particles are surrounded by only MgO (or ZnO) particles. The values of k_A^O and k_B^O decreased with the increase in the calcination temperature of Fe_2O_3. (Japanese)

Bonding of Alumina Ceramic and Nickel Using Active Metal Filler and Cu-W Interlayer
—Part 1—

Toshio Narita and Tatsuo Ishikawa

Reports on the High-Temperature Material in the 123rd
Division of JSPS, Vol. 28 (No. 2), 1987, 233-238

Alumina ceramics and nickel were joined using a Ti-Cu-Ag filler and Cu-W interlayers at 1173 K for 1.8 ks. Direct bonding of alumina to nickel without the interlayer was unsuccessful because of the high thermal residual stress due to the expansion mismatch.

Using a Cu-W interlayer the sound bondings were made, and the maximum fracture strength was obtained to be 160 MPa (four point bending strength), when using Ti-foil of 1.5-5.0 μm, Cu plate of 0.7-1.0 mm and W plate of 2 mm. Dependence of the fracture strength on the Cu and W plate thickness were explained reasonably basing on the FEM calculation. (Japanese)

Bonding of Si_3N_4 Ceramics and an Fe-26Cr Alloy Using Titanium Foils and a Nickel Interlayer

Toshio Narita, Kazuma Miura, Ahihiro Kumatoritani,
Tatsuo Ishikawa and Ryukichi Nagasaki

Memoirs of the Faculty of Enginneering, Hokkaido University
Vol. 75 (No. 2), 1987, 155-165

A silicon nitride ceramic and an iron-26 mass% chromium alloy was bonded in an argon gas stream using a Ti-foil (20 μm) and Ni plate (1 mm). The fracture strength, obtained by bending tests at room temperature, was approximately 70 MPa for the bondings as-made at 1423 K for 3.6 ksec. By increasing the diffusion-annealing times the strengths were reduced rapidly, resulting in 40 MPa for 32 ksec, and then increased gradually up to 80 MPa for the bondings diffusion-annealed at 1373 K for 360 ksec.

The bonding layer was composed of two layers: One of them is an intermediate layer consisting of the TiN, Ti (Si, Ni), and oxides contained in the ceramics as the binder. The other is the intermetallic compounds such as TiNi, $TiNi_3$, and their mixture, as well as the Ni-Ti solid solution layers.

With the diffusion-annealing at high temperatures the TiNi layer was decomposed to the $TiNi_3$ and then to the Ni (Ti). In accordance with the decrement of the alloy layer thickness the fracture strengths were increased, in particular when the TiNi layer was thinned less than a few micronmeters.

It was found that the high fracture strengths were obtained for the surface-polished bondings, and were more than 200 MPa. This indicates that the surface flaws reduced significantly the fracture strength of the as-bonded specimens. (English)

The Structure of the Uranyl Chloro-Complex Determined with the Stability Constants

Hiroshi Ohashi and Takashi Morozumi

Bulletin of the Faculty of Engineering, Hokkaido University,
No. 135, 73-76 (1987)

The theory of ion pair formation, the outer-sphere complexation theory, for a dumbbell configuration of the uranyl ion was used to explain the ionic strength dependence of the stability constant of uranyl chloro-complex. In this model, it was assumed that the chloride ion interacted electrostatically with each of the uranium and oxide ions, and the distance was evaluated to be 0.3 nm between the uranium and chloride ions. This distance suggests that one of the water molecules coordinating with the uranium ion is replaced by a chloride ion and that a complex of the type $UO_2(H_2O)_3Cl^+$ is formed. One chloride ion and three water molecules coordinate around the uranium ion in the same plane, perpendicular to the long axis of the uranyl ion dumbbell. A semiempirical equation, $K_{OS}=0.0681 \exp [1815/\{1+17.05 (I/T)^{1/2}\}T]$, was determined for the stability constant of the uranyl chloro-complex as a function of the ionic strength, I, and temperature, T. (Japanese)

Paramagnetic Cobalt (III) Complexes with Organic Ligands. X. The Preparation and Properties of Radical Diamminebis-(5-nitrosalicylideneaminato) cobalt (III) Complex and Biradical Diamminebis(5-nitrosalicylideneaminato) cobalt (II) Complex

Yoshihisa Yamamoto and Hidetaka Konno

Bull. Chem. Soc. Jpn., **60**, 1299–1302 (1987)

From the reaction mixture of diamminebis(salicylideneaminato) cobalt (III) complex, 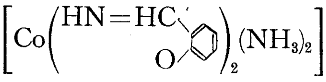

(**1**) and 60% nitric acid, radical diamminebis(5-nitrosalicylideneaminato) cobalt (III) complex, 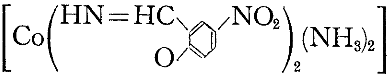

(**2**), and biradical diamminebis(5-nitrosalicylideneaminato)cobalt (II) complex, 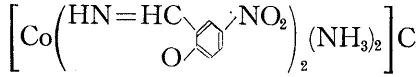

(**3**), have been isolated and characterized by analytical, magnetic, spectroscopic, and XPS methods. The effective magnetic moments of **2** and **3** were 1.7 and 5.5 BM, respectively. In the IR spectrum of **2**, a band due to the rocking deformation vibration of NH_3 was observed at ca. 840 cm^{-1}. The absorption spectra of **2** and **3** showed a strong absorption peak at ca. 690 nm. In the XPS, Co 2p spectra for **3** showed strong satellites, indicating the oxidation number of the cobalt to be +2, whereas no satellites were observed for the other complexes. In comparison with diamagnetic cobalt (III) complex, 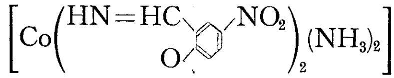

(**4**), C 1s spectra for **2** and **3** showed much larger shoulders on the higher binding energy side due to the electron-poor carbons. It suggests the presence of an unpaired spin on ligands in accordance with paramagnetism of the complexes. (English)

Ylide-Metal Complexes. XIII. An X-Ray Photoelectron Spectroscopic Study of Bis(dimethylsulfoxonium methylide)gold Chloride

Hidetaka Konno and Yoshihisa Yamamoto

Bull. Chem. Soc. Jpn., **60**, 2561-2564 (1987)

Bis(dimethylsulfoxonium methylide)gold chloride, $[(CH_3)_2S(O)CH_2\text{-}AuCH_2S(O)(CH_3)_2]Cl$, has been studied by X-ray photoelectron spectroscopy. The C 1s spectrum was separated into two peaks at $E_B=284.0$ and 285.1 eV in a ratio of 1 : 2. The peak at 285.1 eV corresponds to the methyl carbons, and that at 284.0 eV is assigned to the electron-rich methylene carbon (or carbanion). The E_B of Cl $2p_{3/2}$ agreed with that for chlorobis(triphenylphosphine)gold(I) and chlorobis(triphenylmethylenephosphorane)gold(I). The E_B of Au $4f_{7/2}$ was 84.4 eV, suggesting the oxidation number +1. These results indicate that the structure of the title complex is $(CH_3)_2\text{-}S(O)CH_2Au(Cl)CH_2S(O)(CH_3)_2$, and different from that reported previously. (English)